Available online at www.sciencedirect.com
SCIENCE DIRECT®
Bioorganic & Medicinal Chemistry 13 (2005) 5181–5188
Bioorganic & Medicinal Chemistry

The solution structure of a lasalocid A metal complex in lipophilic solvents☆

Silvia Ripoli, Simona Scarano, Lorenzo Di Bari and Piero Salvadori*

CNR-ICCOM sez. di Pisa, Dipartimento di Chimica e Chimica Industriale, via Risorgimento 35, 56126 Pisa, Italy

Received 13 April 2005; revised 5 May 2005; accepted 5 May 2005
Available online 1 July 2005

Abstract—Lasalocid A (LasNa), a common antibiotic in veterinary medicine, is a polyetheral ionophore, disrupting cation equilibria through the cell wall. By means of circular dichroism (in the UV and in the near-IR), paramagnetic NMR, and with the aid of the program PERSEUS, we determined the solution geometry of the 1:1 Las–Yb^{3+} complex in CD_3CN and $CDCl_3$, following a protocol similar to the one successfully used for the anthracycline–metal adduct. The resulting structure is in full agreement with the expectation of the ligand wrapping around the cation in a horseshoe shape. The oxygen atoms participate in the coordination either through a direct, first sphere, or a longer range interaction.

1. Introduction

Lasalocid A (LasNa, Fig. 1) is one of the most commonly used veterinary antibiotics, where it has found widespread application as anticoccidial and to improve feed efficiency. The mechanism of action of lasalocid is clearly attributed to its ionophoric properties, because it has been reported to determine the influx of Na^+ in the cell of gram positive and anaerobic bacteria, causing swelling, vacuolization, and death. At the origin of these processes, there is the property of forming lipophilic metal complexes, which can penetrate membranes and disrupt cation equilibria.[1,2]

While these aspects have been clarified, the molecular basis of this action are still debated, more specifically which of the oxygen atoms are directly involved in cation coordination. To date, this problem has been the object of many investigations almost invariably taking advantage of the concerted use of several experimental and computational techniques, which demonstrates both the relevance of the problem and its intrinsic difficulty.[3] The identity of the various complexes formed according to the nature of the cation, to the solvent, and to the solution composition has been initially faced with optical spectroscopy and circular dichroism (CD), possibly using lanthanides as probes.[4] X-ray diffraction data became available for several cations, among others Na^+,[5] and Ba^{2+}.[6] Often, it has been observed that aggregates of different stoichiometry can take place, leading to the formation of sandwiches, where the cation occupies a cavity between two ligand molecules.[3] Molecular dynamic calculations have been reported both in vacuo[7] and in solvent.[8] Finally, there has recently appeared a series of papers on polyoxaalkyl lasalocid esters/cation complexes making use of multinuclear NMR, IR, ESI-MS, and semiempirical methods.[9]

We approached the problem following the lines of a previous investigation on anthracyclins/metal complexes, by means of paramagnetic NMR and CD, with ytterbium as both the cation and the structural probe.[10]

The ^1H and ^{13}C NMR spectra of Yb^{3+} complexes feature a signal spreading, determined by the large pseudocontact interaction, on top of the usual chemical shielding and together with the small and often negligible contact interaction.[11] These three interactions lead to additive contributions to the shift, that can be named δ^{PC}, δ^{dia}, and δ^{C}, respectively. We shall assume $\delta^{C} = 0$, which leads for each nucleus i, to

$$\delta_i^{PC} = \delta_i - \delta_i^{dia} = D_1 \frac{1 - 3\cos^2\theta}{r_i^3} + D_2 \frac{\sin^2\theta \cos 2\varphi}{r_i^3}. \quad (1)$$

Keywords: Chirality; Lanthanides; Paramagnetic NMR; Ionophores; Lasalocid A.

☆ In honour of Professor Koji Nakanishi, recipient of the Tetrahedron Prize 2004.

* Corresponding author. Tel.: +39 050 221 9273; fax: +39 050 221 9409; e-mail: psalva@dcci.unipi.it

0968-0896/$ - see front matter © 2005 Published by Elsevier Ltd.
doi:10.1016/j.bmc.2005.05.034

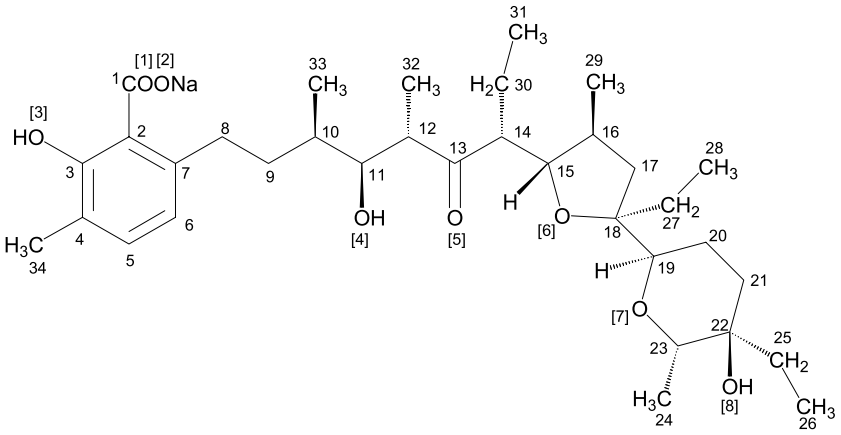

Figure 1. Structure and atom numbering of LasNa. Oxygen atoms are labeled within square brackets.

In this equation according to a well-known formalism,[11] D_1 and D_2 are combination of the components of the anisotropic part of the magnetic susceptibility tensor; r_i is the distance of the nucleus from the paramagnetic ion and finally θ and φ indicate the orientation of the $\vec{r}$ vector with respect to the principal axes of the magnetic susceptibility tensor. The difference indicated in Eq. 1, $\delta_i - \delta_i^{\text{dia}}$, is often called lanthanide-induced shift or LIS. It is most correctly estimated by taking the observed shift difference between a paramagnetic Yb^{3+} and a dimagnetic Lu^{3+} isostructural complexes with the same ligand. However, at least for Yb^{3+} identifying δ_i^{dia} with the shift of the nucleus in the free, uncomplexed ligand leads to a minor error.

Apart from LIS, there is a remarkable enhancement of both longitudinal and transverse nuclear relaxation rates, leading to a lanthanide-induced relaxation (LIR) effect, which can be measured, for example, by inversion recovery. Once again, one must take the difference between the rates of the nuclei in the paramagnetic complex and in the free ligand. The LIR is linked to the nucleus–Yb^{3+} distance r_i, through the equation

$$\rho_i^{\text{LIR}} = \frac{C}{r_i^6}, \tag{2}$$

where C is a proportionality constant depending on the electronic and rotational correlation times and which will be discussed further below.

Clearly both δ^{PC} and the LIR contain structural information, which can define the molecular conformation of the adduct. We developed the program PERSEUS as a tool for decoding the geometrical parameters embedded in the experimental ^1H and ^{13}C NMR data.[10,12]

As useful complement to the magnetic properties, Yb^{3+} offers a further spectroscopic tool, namely an *f–f* electronic transition ($^2F_{7/2} \rightarrow {}^2F_{5/2}$) whose energy gravity center falls in the near infrared (NIR) around 980 nm. The CD bands, induced by a dissymmetric ligand field, associated to this transition can be easily observed on a suitable spectropolarimeter.[13] Consequently, one can take advantage of NIR CD spectroscopy, which responds only to chiral non-racemic ytterbium complexes.[14]

2. Results

2.1. Spectroscopic measurements

The existence of an NIR CD spectrum of a mixture of LasNa and $Yb(OTf)_3$ in CH_3CN indicates clearly the formation of a chiral complex between the lanthanide ion and lasalocid (Fig. 2). This spectrum shows a structured shape, characterized by two negative bands (997 and 966 nm) and two positive bands (976 and 928 nm) with a shoulder around 940 nm. Because NIR CD spectroscopy is sensitive only to dissymmetric Yb^{3+} complexes, it was possible to follow the formation of Las^-–Yb^{3+} by monitoring the evolution of the CD spectrum. Following the addition of LasNa to a solution of

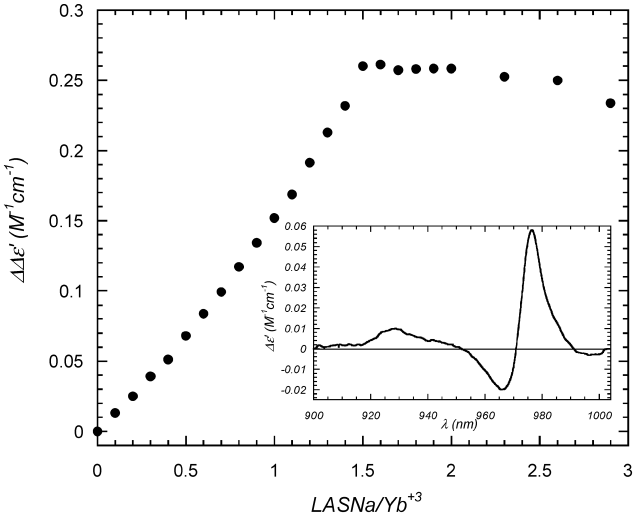

Figure 2. Molar ratio plot relative to the NIR CD titration of Yb^{3+} in CH_3CN with LasNa (method II reported in Section 5); $\Delta\Delta\varepsilon' = (\Delta\varepsilon'_{976} - \Delta\varepsilon'_{966})$, where $\Delta\varepsilon'_\lambda$ is the differential absorption normalized to the total concentration of Yb^{3+}. In the inset, the NIR CD spectrum of the Las^-–Yb^{3+} complex in CH_3CN is reported ([Yb^{3+}] = 17.8 mM; [LasNa] = 9.3 mM).

Yb^{3+} (performed in triplicate, see Section 5), the intensities of all the CD bands vary linearly with increasing the molar ratio up to [LasNa]/[Yb^{3+}] = 1.5 afterwards, the intensity stabilizes. The sharp change of trend in the dichroic intensity versus molar ratio (Fig. 2) and the presence of several isosbestic points (all with $\Delta A = 0$) show that only one complexed species is present in solution.

The addition of Bu_4NPF_6 (usually used as supporting electrolyte)[15] to a solution of $Yb(OTf)_3$ in CH_3CN prevents the formation of the Las^-–Yb^{3+} complex, in fact it is impossible to detect any CD bands of Yb^{3+} in its presence. Because it is known that lasalocid binds ammonium groups through carboxylate,[3,16] this may indicate that the carboxylic moiety has a crucial role in metal ligation.

The complete assignment of ^1H and ^{13}C NMR spectra of lasalocid metal complexes are reported in Tables 1 and 2. In the case of diamagnetic LasNa and LasNa/Lu^{3+} systems, a comparison with the literature data[8] and standard two-dimensional (2D) NMR experiments aided the assignment.

Table 1. ^1H NMR spectral assignment of metal complex of lasalocid in acetonitrile or in chloroform and experimental longitudinal relaxation times (T_1) measured for the ytterbium complex

H_i	CD_3CN				$CDCl_3$
	LasNa	Las^-–Lu^{3+}	Las^-–Yb^{3+}		Las^-–Yb^{3+}
	δ (ppm)	δ (ppm)	δ (ppm)	T_1 (ms)	δ (ppm)
5	6.94	7.08	6.22	420	6.17
6	6.45	6.56	11.14	136	11.30
8A	2.18	2.25	23.13	29	24.12
8B	3.81	3.85	55.96	3	60.22
9A	1.40	2.03	17.57	34	16.97
9B	1.58	1.56	24.55	6	22.54
10	1.70	2.02	41.33	18	40.82
11	4.26	4.60	—	—	—
12	2.89	3.26	26.63	10	24.12
14	2.78	3.21	8.60	37	7.33
15	3.70	3.66	−11.35	30	−9.86
16	2.20	2.31	−3.72	104	−4.45
17A	1.87	1.93	−4.63	202	−4.65
17B	1.39	1.42	−8.10	155	−8.10
19	3.56	3.47	−6.25	147	−6.75
20A	1.77	1.49	−32.70	29	−34.06
20B	1.43	1.53	−12.36	115	−12.26
21A	1.28	1.55	−11.80	110	−13.20
21B	1.68	1.50	−6.98	97	−7.66
23	3.73	3.59	7.44	29	—
24	1.08	1.05	−1.24	160	−2.34
25A	1.68	1.33	−6.87	170	−7.66
25B	1.78	1.74	−7.65	57	−7.66
26	0.70	0.77	−3.36	118	−3.60
27A	1.80	0.99	−3.60	94	—
27B	1.29	1.08	−1.03	138	—
28	0.84	0.42	1.76	210	1.48
29	0.99	1.08	−1.58	205	−1.25
30A	1.78	2.12	−13.40	17	−17.24
30B	1.29	1.54	−3.82	63	−5.33
31	0.80	0.90	2.68	40	1.48
32	0.92	1.26	31.32	24	30.79
33	0.80	1.02	11.28	35	10.06
34	2.00	2.07	−1.32	442	−1.40
O[3]H	15.84[a]	13.74[a]		—	
O[4]H	4.86[b]	9.86[d]	−21.00	—	−26.33
O[8]H	6.44[c]	6.65[c]	−96.70	—	−94.04

Labels A and B indicate *pro-S* and *pro-R* protons, respectively.

Table 2. ^{13}C NMR spectrum assignment (δ, ppm) of metal complexes of lasalocid in acetonitrile

C_i	Las^-–Lu^{3+}	Las^-–Yb^{3+}
4	115.1	—
5	134.6	133.4
6	122.1	123.7
7	145.5	—
8	34.3	64.1
9	27.1	71.5
10	33.8	86.4
11	72.5	—
12	48.8	118.2
14	53.6	51.3
15	86.1	70.1
16	36.3	27.6
17	38.1	28.2
18	87.4	—
19	70.7	54.0
20	20.6	0.8
21	30.7	17.0
22	89.2	—
23	76.4	69.9
24	14.4	11.6
25	30.5	20.3
26	9.7	6.5
27	32.4	27.6
28	6.0	6.0
29	15.9	11.0
30	17.5	11.7
31	12.9	13.2
32	13.5	38.5
33	13.8	30.3
34	31.0	11.4

The stepwise addition of paramagnetic Yb^{3+} to LasNa in CD_3CN determines the progressive disappearing of the LasNa proton resonances and the appearance of new signals, which span a spectral width from 60 to −90 ppm. Around [LasNa]/[Yb^{3+}] = 0.9, the signals of LasNa are practically undetectable and the ^1H NMR spectrum does not evolve further. No decoalescence of proton signals at low temperature (T_{min} = 233 K in CD_3CN and T_{min} = 253 K in $CDCl_3$) was found. Thus, the final spectrum obtained during the metal titration can be attributed to the only paramagnetic complex Las^-–Yb^{3+}.[17]

The EXSY spectrum (see 'Supplementary data') recorded for Las^-–Yb^{3+} puts an upper limit to the rate of the exchange between free and bound forms: $k \ll 2000\ s^{-1}$. Remarkably, working with a molar ratio [Las^-]/[Yb^{3+}] = 0.9 and notwithstanding the small molar fraction of free lasalocid (due to a high binding constant)[4b] it was possible to acquire a full EXSY spectrum.

The EXSY spectrum, in conjunction with COSY and TOCSY data, allowed the assignment of ^1H NMR spectrum of Las^-–Yb^{3+} in acetonitrile, shown in Table 1 and Figure 3. The signals at −21.00 and −96.70 ppm were

attributed to two hydroxyl groups, because they disappeared after addition of D_2O to the sample. Finally, the assignment of H-11 and ethyl groups (H-25, H-26) and (H-27, H-28) remained ambiguous, as will be discussed below. Once the proton spectra assignment was completed, HETCOR and HMQC allowed us to assign most carbon resonances of Las^{-}–Yb^{3+} in CD_3CN. In Table 1, the ^1H longitudinal relaxation times of the Las^{-}–Yb^{3+} complex are also reported.

Because of the low solubility of ytterbium salts in chloroform, spectroscopic experiments in this solvent resulted more difficult. However, the ^1H NMR spectrum of Las^{-}–Yb^{3+} in $CDCl_3$ (Table 1 and 'Supplementary data') is very similar to that in CD_3CN, so the full assignment in the former solvent was realized through correlation to the data in acetonitrile, by means of the titration described in Section 5.

2.2. Structure determination

A first set of proton–ytterbium distances (r) were derived from Eq. 2 using the longitudinal relaxation rates measured through inversion recovery $\rho^{LIR}_{1,i} = C/r_i^6$ ($\rho^{LIR}_{1,i} = \rho^{obs}_{1,i} - \rho^{dia}_{1,i}$, after reasonably setting $\langle\rho^{dia}_{1,i}\rangle = 2\ s^{-1}$ for all protons); C is a phenomenological constant containing a linear combination of electronic and rotational correlation times. At this stage, a value of 1.5×10^5 Å^6 s^{-1} for C was deduced from the literature.[11]

These calculated distances were used in an MM2 geometry optimization as constraints to obtain a first tentative structure of the ytterbium complex, starting from an unfolded conformation of lasalocid. This resulted in an initial set of ligand coordinates, to perform a fitting through the program PERSEUS.[10,12] This program optimizes the paramagnetic ion location, minimizing the mean square residual between calculated and experimental relaxation rates and/or pseudocontact shifts, estimating the components of the anisotropic magnetic susceptibility tensor and the constant C. This process was iteratively repeated up to convergence of the C value, using the data reported in Table 3, excluding ethyl groups. This structure of the complex was further refined by optimizing the conformation of ethyl groups (H-26, H-25) and (H-28, H-27), whose experimental NMR data were introduced in the input set for PERSEUS, in order to find the optimal dihedral angle which fixes their conformation. During this phase, the assignment ambiguity for (H-26, H-25) and (H-28, H-27) was solved. A final $C = (3.1 \pm 0.5) \times 10^5$ Å^6 s^{-1} was estimated. The ultimate structure is reported in Figure 4 where the values and orientation of the magnetic anisotropy tensor are also shown.

To test the reliability of the geometry calculation, of the 83 experimental data only 53 values were inserted into the fitting (Table 3) and the rest was used as control (Table 4). The optimization can be considered accurate because about the 60% of all unused had a residual less than 4.00 ppm for the shifts and less than 1.2 Å for the distances. It must be noticed that most of the inaccurate shift values correspond to nuclei for which contact shift might be non-negligible; the estimated proton–ytterbium distances evaluated through $\rho^{LIR}_{1,i}$ are instead satisfactory, also for H-12, whose shift is imprecise. Finally, for the H-11 $\delta^{PC} = 303$ ppm was calculated, according to the very small distance of this proton from the paramagnetic cation in the optimized structure. Because of the extremely large shift and of the estimated linewidth (0.1 MHz), it is not surprising that its signals cannot be detected in the NMR spectrum.

It must be noticed that the X-ray structure[6,18] of the barium adduct is unsatisfactory as input for PERSEUS. This indicates that it differs from that of the Yb^{3+} adduct in solution. Particularly, the exposure to the cation of the oxygen atoms O[5], O[6], and O[7] is different (Fig. 5).

In the proposed structure of Las^{-}–Yb^{3+} (Fig. 4), two groups of coordinating oxygens can be distinguished. To a first sphere, closer to Yb^{3+} ($\langle r_{O-Yb}\rangle = 3$ Å) belong carboxyl, O[5], and O[8], whereas to an outer sphere

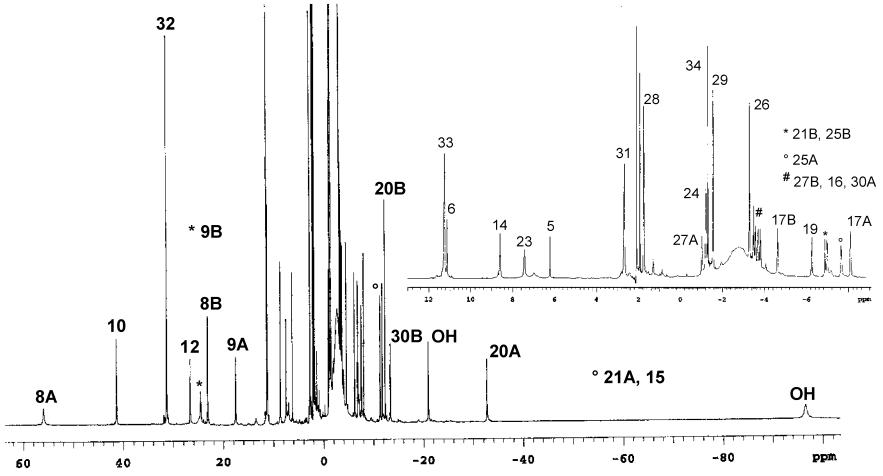

Figure 3. ^1H NMR spectrum of the paramagnetic Las^{-}–Yb^{3+} complex in CD_3CN with the spectrum assignment indicated by the labels. The vertical scale of the expansion is the 28% of that of the full spectrum.

Table 3. Calculated values of the ^{13}C, ^{1}H shifts (δ_{calc}, ppm) and proton–ytterbium distance ($[r_{H-Yb}]^{calc}$, Å) inserted as experimental constraints in the PERSEUS fitting

C_i	^{13}C		H_i	^{1}H			
	δ_{calc}	$\delta_{calc} - \delta_{exp}$		δ_{calc}	$\delta_{calc} - \delta_{exp}$	$[r_{H-Yb}]^{calc}$	Δr_{H-Yb}
5	135.2	1.8	5	7.76	1.54	8.5	−1.0
6	125.2	1.5	6	11.23	0.09	6.7	0.6
8	61.7	−2.4	8A			4.7	0.2
9	72.0	0.5	8B			3.2	0.1
15	71.1	1.0	9A	17.01	−0.56	5.2	1.2
16	28.6	1.0	9B	21.71	−2.84	3.7	0.2
17	28.4	0.2	10			4.5	0.3
20	−3.5	−4.3	14			5.5	0.8
			15			4.6	0.1
			16	−3.72	0.00	6.5	0.8
			17A	−4.26	0.37	7.3	0.5
			17B	−7.83	0.27	6.5	0.2
			19	−7.37	−1.12	6.1	−0.1
			20A	−34.66	−1.96	4.3	−0.2
			20B	−12.18	0.18	6.0	0.1
			21A	−9.79	2.01	6.4	0.6
			21B			5.5	−0.1
			23	7.12	−0.32		
			24	−1.48	−0.24		
			25A	−7.38	−0.51		
			25B	−7.68	−0.03		
			26	−1.07	2.29		
			27A	−4.76	−1.16		
			27B	−3.10	−2.07		
			28	−2.36	−4.12		
			29	−1.30	0.28		
			30A	−13.13	0.27	4.2	0.1
			30B	−4.93	−1.11	5.8	0.6
			31	−4.29	−6.97		
			32	21.98	−9.34		
			33	14.81	3.53		
			34	1.27	2.59		

($\delta_{calc} - \delta_{exp}$) is the residual between calculated and experimental shifts, whereas Δr_{H-Yb} corresponds to ($[r_{H-Yb}]^{calc} - [r_{H-Yb}]^{0}$), where $[r_{H-Yb}]^{0}$ are proton–ytterbium distances in the complex structure optimized by iterative process with MM2 and PERSEUS.

($\langle r_{O-Yb} \rangle$ = 4 Å) belong O[4], O[6], and O[7]; instead O[3] appears completely non-coordinating.

The structure of Figure 4 was used as a basis for the analysis through PERSEUS of ^{1}H shifts measured at low temperature, determining the magnetic susceptibility tensor at 273, 253, and 233 K (see 'Supplementary data'). No significant changes in the values and orientations of the tensor components were found; moreover, the average residuals, $\langle|\delta^{PC} - \delta^{PC}_{calc}|\rangle$, were found similar at the different temperatures: 0.84 ppm (298 K); 0.94 ppm (273 K); 0.81 ppm (253 K); and 0.82 ppm (233 K).

These further calculations indicate that the PERSEUS structure is representative of the most stable conformation in solution. Thus, room temperature equilibria involving relevant conformational rearrangements can be excluded.

3. Discussion

The results obtained shed new light on the metal–lasalocid interaction. Indeed, through NMR titration we derive that lasalocid forms a 1:1 complex with Yb^{3+}. The NIR CD demonstrates the existence of one complex, consistently with NMR, although the stoichiometry suggested by the molar ratio plot can hardly be interpreted.[17]

All the NMR spectra are compatible with one Las^{-}–Yb^{3+} species, with only one form of bound lasalocid. The possibility of larger aggregates, involving more metal ions and more ligands, is ruled out by the low temperature ^{1}H NMR spectra, which exclude that the existence of one set of ^{1}H and ^{13}C peaks is due to a dynamic symmetrization process.

The three-dimensional structure of the Las^{-}–Yb^{3+} complex obtained by computational analysis of NMR data shows that carboxyl, O[5], and O[8] are closer to the ion, so they can be considered the principal coordinating groups. The involvement of carboxyl in the cation coordination is also suggested by the experimental observation that an ammonium salt, known to bind lasalocid carboxyl,[3,16] precludes the detection of NIR CD of Las^{-}–Yb^{3+}. On the other hand, it is expected that the trivalent lanthanide ions are characterized by strong affinity constants for negative oxygens,[19] hence the interaction with carboxyl and the replacement of Na^{+}

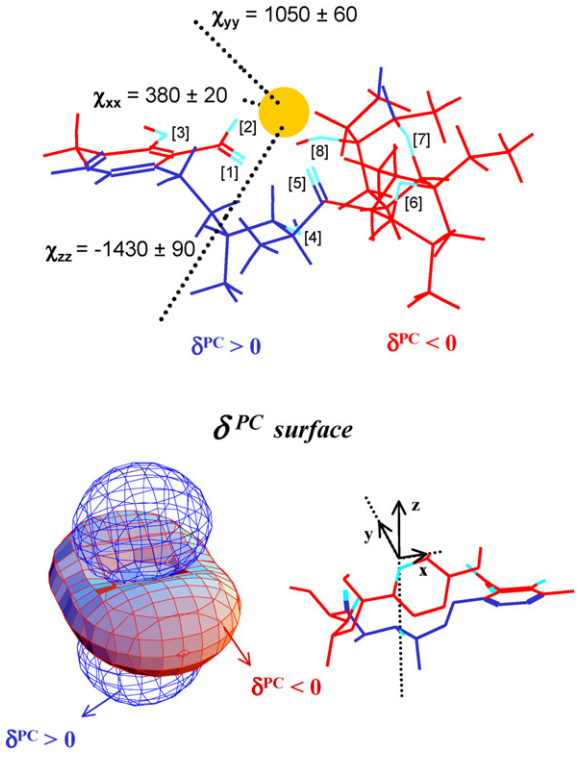

Figure 4. Three-dimensional structure of the Las^{-}–Yb^{3+} complex elicited by NMR data analysis. Atoms with positive pseudocontact shifts ($\delta^{PC} > 0$) are colored in blue, those with negative pseudocontact shifts ($\delta^{PC} < 0$) are in red; oxygen atoms, labeled within square brackets, are in light blue; Yb^{3+} is in yellow. χ_{xx}, χ_{yy}, and χ_{zz} are the components of the anisotropic part of the magnetic susceptibility tensor in the principal axes reference (x, y, z) centered on the paramagnetic ion; the corresponding values were estimated through the optimization by means of PERSEUS. On the bottom the pseudocontact surface in the principal reference (x, y, z) centered on Yb^{3+} (placed on the intersection of the two lobes) is drawn: the red solid lobe is the equi-δ^{PC} surface for negative values; the blue mesh is the equi-δ^{PC} surface for positive values. On the right, the orientation of the complex with respect to the δ^{PC} surface is reported.

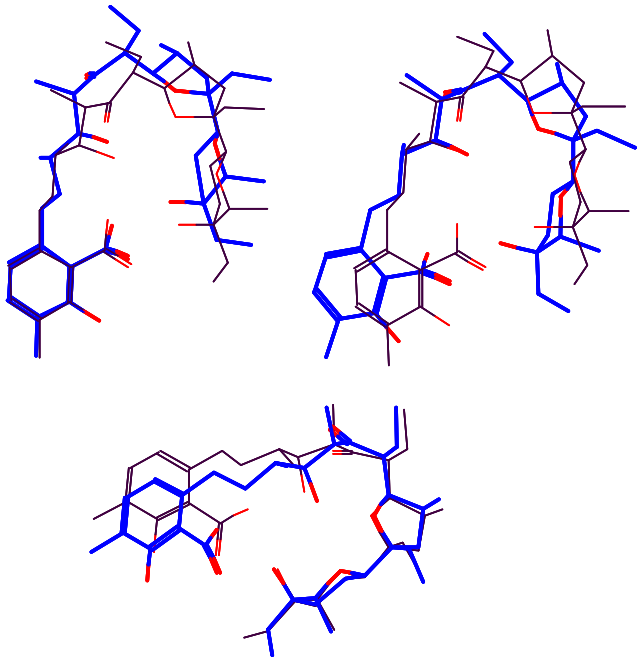

Figure 5. Comparison between X-ray (black)[5] and PERSEUS (blue) structures of metal–lasalocid adducts in three different projections.

is likely. Moreover, since the lanthanides are engaged in mostly electrostatic interactions, it can be hypothesized that O[4], O[6], and O[7] somehow contribute to the coordination of Yb^{3+}, even though they are located farther from the cation. The O–Yb^{3+} distances, longer than those found in typical X-ray structures, may be accepted on account of the probable involvement of the solvent or the counter-ions and of the high adaptability of the ligand to fit the solvated cation in solution.

In literature, except for a report on Gd^{3+}/Mn^{2+}–lasalocid complexes,[20] there is a general uniformity in consid-

Table 4. Calculated values of the ^{13}C, ^{1}H shifts (δ_{calc}, ppm) and proton–ytterbium distance ($[r_{H-Yb}]^{calc}$, Å) not used as experimental constraints in the PERSEUS fitting

C_i	^{13}C		H_i	^{1}H			
	δ_{calc}	$\delta_{calc} - \delta_{exp}$		δ_{calc}	$\delta_{calc} - \delta_{exp}$	$[r_{H-Yb}]^{calc}$	Δr_{H-Yb}
10	83.8	−2.6	8A	25.67	2.54		
12	85.6	−32.6	8B	41.69	−14.27		
14	46.7	−4.6	10	49.82	8.49		
19	50.4	−3.6	12	18.71	−7.92	5.0	1.2
21	10.9	−6.1	14	2.24	−6.36		
23	65.4	−4.5	15	−7.60	3.75		
24	10.7	−0.9	21B	−15.83	−8.85		
25	20.7	0.4	23			5.5	1.0
26	6.4	−0.1	25A			6.6	0.2
27	25.0	−2.6	25B			5.6	0.5
28	2.4	−3.6	27A			6.3	0.7
29	12.6	1.6	27B			5.2	−0.9
30	7.7	−4.0					
31	7.0	−6.2					
32	38.7	0.2					
33	32.8	2.5					
34	30.2	18.8					

($\delta_{calc} - \delta_{exp}$) is the residual between calculated and experimental shifts, whereas Δr_{H-Yb} corresponds to ($[r_{H-Yb}]^{calc} - [r_{H-Yb}]^{0}$), where $[r_{H-Yb}]^{0}$ are proton–ytterbium distances in the complex structure optimized by iterative process with MM2 and PERSEUS.

ering O[5], O[6], and O[7] as being directly involved in the coordination of the cation.[4,21] Some contrasting results are instead reported for the involvement of O[4], O[8], and the carboxylate group. Our findings reveal that, excluding O[3], all oxygens contribute somehow to the coordination of Yb^{3+} probably creating an electrostatic interaction sphere.

Interestingly, we can follow the evolution of the ^1H NMR spectrum on going from pure acetonitrile to pure chloroform and the position of all the lines remains practically identical (within a few ppm). This observation demonstrates that the conformation of the complex remains practically intact in two quite different media: a polar solvent like CD_3CN ($\varepsilon = 37.5$) and a completely apolar one like $CHCl_3$ ($\varepsilon = 4.8$). This demonstrates that the structure we obtained can be regarded as truly representative of the adduct in lipophilic media, like cell membranes.

4. Conclusions

NIR CD makes immediately evident the formation of a chiral adduct between lasalocid and Yb^{3+}: the organic ligand is silent in NIR, while Yb^{3+} alone (or coordinated with achiral ligands) cannot give rise to Cotton effects. Thus, this spectroscopic technique is ideal for following the formation of the complex.

The quantitative investigation of the molecular structure in true apolar media was hampered by the sparing solubility of Yb^{3+} salts. On the other hand, the ^1H NMR spectra of Las–Yb in chloroform and acetonitrile are practically identical, which ensures that the adduct does not change conformation in the two organic solvents in spite of the large difference in polarity. In the latter solvent, a set of 2D spectra allowed us to completely assign the proton and carbon resonances and to determine the pseudocontact shifts for a large set of nuclei. The spectroscopic information was further completed by ^1H longitudinal relaxation rates. The complete set of data was largely redundant for structural optimization; this allowed division of the data into two subsets: one was used as input for the program PERSEUS, while the other served as an independent check for consistence of the resulting data (geometrical parameters as well as the magnetic susceptibility tensor).

Lasalocid folds around the cation, providing a polar cavity, while offering an apolar surface to the solvent. This ensures efficient cation transport in apolar media. It is interesting to observe that the carboxylate oxygen do not appear engaged in cation coordination. Thus, one can expect a similar structure also for the complexes where the ligand is an ester derivative of lasalocid. It is interesting to observe that, in spite of the several degrees of freedom ensured by the C–C bonds, the complex Las–Yb is rather stiff. We can tentatively extend this information to other metal adducts of this important ionophore, most notably to calcium.

5. Experimental

Lasalocid A sodium salt (LasNa in the text) was used as the Fluka product (degree of purity $\geqslant 97\%$); lanthanide chlorides ($YbCl_3$, $LuCl_3$) or trifluoromethanesulfonate ($Yb(OTf)_3$) were anhydrous commercial products (Alfa, degree of purity $\geqslant 97\%$). Tetrabutylammonium hexafluorophosphate was an ABCR product (degree of purity $\geqslant 98\%$).

The NIR CD spectra of Yb(III) were detected at room temperature on a Jasco J200D spectropolarimeter, operating between 750 and 1350 nm, modified by a tandem detector Si/InGaAs with dual photomultiplier amplifier and, if not differently specified, using a 'semimicro' square cell with an optical path of 1 cm.

The optical titrations were carried out in triplicate.

(a) To 1 mL of $Yb(OTf)_3$ (5.0 mM) in CH_3CN, aliquots of 32 μL of LasNa (15.6 mM) in CH_3CN were added up to $[LasNa]/[Yb^{3+}] = 2.9$. A 'macro' square cell (optical path: 1 cm) was used. The spectra were recorded at 50 nm/min with a sensitivity of 1, 2, and 5 m°/cm for $[LasNa]/[Yb^{3+}]$ ranges 0.0–0.8, 0.9–1.4, and 1.5–2.9, respectively. The time constant was 0.5 s, the bandwidth 3.2 nm, and the gain 20; 16 or 8 repeat times for low or high $[LasNa]/[Yb^{3+}]$ were performed, respectively. The concentration of LasNa solution was spectrophotometrically determined, using $\langle\varepsilon\rangle_{306} = 4600 \pm 100\ M^{-1}\ cm^{-1}$.

(b) Different aliquots of $Yb(OTf)_3$ (7.8 mM) and of LasNa (7.8 mM) in CH_3CN were mixed up to a final volume of 500 μL, in order to obtain variable $LasNa–Yb^{3+}$ ratios up to 3.0. The spectra were recorded at 20 nm/min with a sensitivity of 2 m°/cm, a time constant of 0.5 s, a bandwidth of 4.8 nm, a gain of 5, and eight repeat times.

(c) To 9 mL of $YbCl_3$ (0.4 mM) in CH_3CN aliquots of 179 μL of LasNa (10 mM) in CH_3CN up to $[LasNa]/[Yb^{3+}] = 2.4$ were added. The spectra were recorded using a cylindrical quartz cell (optical path 10 cm), at 50 nm/min with a sensitivity of 1 m°/cm, a time constant of 0.5 s, a bandwidth of 3.2 nm, a gain of 20, and 16 repeat times. For all optical titrations, an average error of ±0.2 for the molar ratio was estimated.

The addition of LasNa (15.6 mM) in CH_3CN to 500 μL of $Yb(OTf)_3$ (5.0 mM) and Bu_4NPF_6 (1 M) in CH_3CN lead to non-detectable NIR CD bands. The same result was also obtained with high excess of ytterbium salt.

The ^1H and ^{13}C NMR spectra were acquired on a Varian VXR 300 and a Varian Inova 600 spectrometer, operating at 7.0 and 14.1 T, respectively. The π/2 pulse for ^1H was of 13 μs (7.0 T) or 6.5 μs (14.1 T). The relaxation interval was 4 s in the case of diamagnetic samples and 1 s for paramagnetic samples. If not otherwise specified, the complex NMR spectra were recorded mixing LasNa and a lanthanide salt in 500 μL of solvent (CD_3CN, $CDCl_3$), obtaining concentrations of 5–10 mM. All experiments, including DQF-COSY (for

diamagnetic samples) and absolute value COSY (for paramagnetic samples)[1] were acquired by means of conventional sequences. The EXSY spectra were detected through the NOESY sequence. The longitudinal relaxation times (T_1) were measured by an inversion–recovery sequence, adequately moving the transmitter in the case of large spectral widths.

The NMR titration was performed adding 5 μL aliquots of $Yb(OTf)_3$ (10 mM) in CD_3CN to a 500 μL solution of LasNa (1.0 mM) up to LasNa–Yb^{3+} ratio 1:1.

The solvent exchange experiment was conducted adding portions of 50 μL of $CDCl_3$ to 400 μL of Las^-–Yb^{3+} (10 mM) in CD_3CN solution until the final volume of 0.8 mL. Similarly, eight aliquots of 50 μL of CD_3CN were added to 400 μL of Las^-–Yb^{3+} in $CDCl_3$. In this way the two sets of spectra were linked up.

The conformation of Las^-–Yb^{3+} complex was obtained by concerted use of an MM2 simulation, available in the software CS Chem3D Pro (version 3.5.2, CambridgeSoft Corporation), and of the FORTRAN routine PERSEUS (paramagnetic enhanced relaxation and shifts for eliciting ultimate structures).[10,11c,12] The pseudocontact surface was drawn through the program Mathematica4 (version 4.0.0.0, Wolfram Research) on the basis of Eq. 1 and the parameters calculated by PERSEUS.

Acknowledgments

The kind help of Prof. Fabio Marchetti in retrieving crystal structures from databases is gratefully acknowledged. This work received financial support from MIUR and CNR.

Supplementary data

EXSY, COSY, HMQC and low temperature spectra of Las^-–Yb^{3+} in CD_3CN; magnetic susceptibility anisotropy tensor at low temperature; ^1H NMR spectrum of Las^-–Yb^{3+} in $CDCl_3$. Supplementary data associated with this article can be found in the online version at doi:10.1016/j.bmc.2005.05.034.

References and notes

1. Crandall, L. W.; Hamill, R. L. In *Kirk-Othmer Encyclopedia of Chemical Technology*; 4th ed. Wiley: New York, 1992; Vol. 3, pp 306–331.
2. Lindsay, D. S.; Blagburn, B. L. In *Veterinary Pharmacology and Therapeutics*; Adams, H. R., Ed.; Blackwell Publishing Professional: Ames, IA, 2001, p 992.
3. Lindoy, L. F. *Coord. Chem. Rev.* **1996**, *148*, 349.
4. (a) Vishwanath, C. K.; Easwaran, K. R. K. *FEBS Lett.* **1983**, *153*, 320–324; (b) Shastri, B. P.; Sankaram, M. B.; Easwaran, K. R. K. *Biochemistry* **1987**, *26*, 4930–4936; (c) Tsukube, H.; Takeishi, H.; Yoshida, Z. *Inorg. Chim. Acta* **1996**, *251*, 1–3; (d) Aguilar-Caballos, M. P.; Gómez-Hens, A.; Pérez-Bendito, D. *Talanta* **1999**, *48*, 209–217.
5. Schmidt, P. G.; Wang, A. H. J.; Paul, I. C. *J. Am. Chem. Soc.* **1974**, *96*, 6189.
6. Johnson, S. M.; Herrin, J.; Liu, S. J.; Paul, I. C. *J. Am. Chem. Soc.* **1970**, *92*, 4428.
7. (a) Malfreyt, P.; Lyazghi, R.; Dauphin, G.; Pascal, Y.; Juillard, J. *J. Chem. Soc., Perkin Trans. 2* **1996**, *85*, 1971–1979, and references cited therein; (b) Tissier, M.; Mousset, G.; Juillard, J. *J. Chem. Soc., Faraday Trans.* **1989**, *2*, 85, 1337–1349 and references cited therein.
8. Lyazghi, R.; Cuer, A.; Dauphin, G.; Juillard, J. *J. Chem. Soc., Perkin Trans. 2* **1992**, 35–42.
9. (a) Pankiewicz, R.; Schroeder, G.; Przybylski, P.; Brzezinski, B.; Bartl, F. *J. Mol. Struct.* **2004**, *688*, 171; (b) Pankiewicz, R.; Schroeder, G.; Brzezinski, B.; Bartl, F. *J. Mol. Struct.* **2004**, *699*, 53; (c) Pankiewicz, R.; Pawlowska, A.; Schroeder, G.; Przybylski, P.; Brzezinski, B.; Bartl, F. *J. Mol. Struct.* **2004**, *694*, 55; (d) Pankiewicz, R.; Pawlowska, A.; Schroeder, G.; Przybylski, P.; Brzezinski, B.; Bartl, F. *J. Mol. Struct.* **2004**, *694*, 155; (e) Pankiewicz, R.; Schroeder, G.; Przybylski, P.; Brzezinski, B. *J. Mol. Struct.* **2005**, *733*, 155; (f) Pankiewicz, R.; Schroeder, G.; Przybylski, P.; Brzezinski, B. *J. Mol. Struct.* **2005**, *733*, 217.
10. Di Bari, L.; Pintacuda, G.; Ripoli, S.; Salvadori, P. *Magn. Reson. Chem.* **2002**, *40*, 396–405.
11. (a) Bertini, I.; Luchinat, C. *Coord. Chem. Rev.* **1996**, *150*, 1–296; (b) Peters, J. A.; Huskens, J.; Raber, D. J. *Prog. Nucl. Magn. Reson. Spectrosc.* **1996**, *28*, 283–350; (c) Di Bari, L.; Salvadori, P. *Coord. Chem. Rev.* **2005**, in press, doi:10.1016/j.ccr.2005.03.006.
12. Di Bari, L.; Lelli, M.; Pintacuda, G.; Pescitelli, G.; Marchetti, F.; Salvadori, P. *J. Am. Chem. Soc.* **2003**, *125*, 5549–5558.
13. (a) Di Bari, L.; Pintacuda, G.; Salvadori, P. *J. Am. Chem. Soc.* **2000**, *122*, 5557–5562; (b) Lisowski, J.; Ripoli, S.; Di Bari, L. *Inorg. Chem.* **2004**, *43*, 1388–1934.
14. Di Bari, L.; Lelli, M.; Pintacuda, G.; Salvadori, P. *Chirality* **2002**, *14*, 265–273.
15. Charbonnière, L. J.; Ziessel, R.; Montalti, M.; Prodi, L.; Zaccheroni, N.; Boehme, C.; Wipff, G. *J. Am. Chem. Soc.* **2002**, *124*, 7779–7788.
16. Lindoy, L. F.; Walker, G. W. *J. Am. Chem. Soc.* **1990**, *112*, 3660–3695.
17. The NMR and NIR CD titrations do not quite agree: optical spectroscopy points towards a stoichiometry more complicated than the 1:1 clearly seen in NMR. Moreover, the UV data of Ref. 4 and subsequent confirmation by us suggest the presence of differently associated species. We do not have a satisfactory explanation for this behavior. With several lanthanides, it has been hypothesized that several adducts with different stoichiometries may coexist, in agreement with the complicated titration curves obtained through spectrophotometry. However, they do not contribute to the ^1H and ^{13}C spectra whose interpretation is discussed below.
18. (a) Maier, C. A.; Paul, I. C. *Chem. Commun.* **1971**, 181–182; (b) Schmidt, P. G.; Wang, H. J.; Paul, I. C. *J. Am. Chem. Soc.* **1974**, *96*, 6189–6191.
19. (a) Evans, C. H. *Biochemistry of the Lanthanides*; Plenum Press: New York, 1990; (b) Cotton, S. *Lanthanides and Actinides*; Oxford University Press: New York, 1991.
20. Hanna, D. A.; Yeh, C.; Shaw, J.; Everett, G. W., Jr. *Biochemistry* **1983**, *22*, 5619–5626.
21. (a) Richardson, F. S.; Gupta, A. D. *J. Am. Chem. Soc.* **1981**, *103*, 5716–5725; (b) Albin, M.; Cader, B. M.; Horrocks, W. de W., Jr. *Inorg. Chem.* **1984**, *23*, 3045–3050; (c) Vishwanath, C. K.; Easwaran, K. R. K. *J. Chem. Soc., Perkin Trans. 2* **1985**, 65–68.